Structure and bonding at metal-ceramic interfaces: Ag/CdO(001)

Fangyi Rao, Ruqian Wu, and A. J. Freeman
Department of Physics and Astronomy, Northwestern University, Evanston, Illinois 60208
(Received 19 September 1994)

Electronic-structure total-energy investigations of the metal-ceramic interface system Ag/CdO(001) show that the preferred adsorption site for Ag is above the O site of the clean CdO(001) surface. The calculated equilibrium interlayer separation between the Ag overlayer and the CdO interface layer is 4.32 a.u. and the binding energy is 0.63 eV/atom. The charge transfer between Ag and the CdO substrate is small (0.02 electrons/atom) and the range of the interface effect on the CdO(001) surface is limited to the interface layer. The interfacial hybridization between the Ag and the O atoms makes a significant contribution to the binding of the Ag/CdO(001) interface.

I. INTRODUCTION

Metal-ceramic interfaces are of practical importance due to their technological applications such as structural, electronic, catalytic, composites, thin-film technology, etc.[1] As a result, this field has attracted growing experimental and theoretical attention. Metal-metal-oxide systems are frequently studied as an important metal-ceramic interface since metal oxides are good candidates as substrates.

Experimentally, Fuchs, Treilleux, and Thevenard[2] investigated thin films of Ag deposited on MgO single crystals or multilayers grown on NaCl or KBr single crystals. They found that Ag thin films are grown epitaxially on the MgO(100) surface. Hoel[3] also reported epitaxially grown Au thin films on the MgO(001) surface. Möller and co-workers[4–6] reported a series of experimental studies of ultrathin Cu films on MgO(100) and MgO(111) substrates prepared by electron-beam evaporation techniques. Structural and electronic studies using low-energy electron diffraction (LEED), Auger electron spectroscopy (AES), electron-energy-loss spectroscopy (EELS), etc. showed that Cu grows epitaxially on MgO(001) and that the initially deposited Cu atoms exist in an ionized state and are bonded to the oxygen atoms. Meanwhile, Johnson and Pepper[7] found that adhesion of the M/MgO interface correlates with the corresponding formation free energy for metal oxide (both increase in the order M = Ag, Cu, Ni, Fe, etc.). This shows the possibility of the existence of d-p bonds in the M/MgO interface between M and O. The structural characteristics of Fe ultrathin films grown on MgO(001) surfaces were studied recently by Park[8] using reflection high-energy electron diffraction (RHEED), x-ray photoelectron diffraction (XPD), and LEED techniques. In contrast to earlier work, they found that the initial growth mode of Fe films is not layer by layer. In contrast, Chan, Jang, and Seidman[9] used the atom-probe field-ion microscopy (APFIM) technique to study the Ag/CdO(222) interface. Their results showed, however, that the Ag/CdO interface is atomically sharp, and the sequence of planes through the interface is Ag|O|Cd|. . . .

Theoretical calculations for metal–metal-oxide interfaces have been reported by a few groups. The first *ab initio* study on a metal-ceramic interface, Ag/MgO(001), was reported by Freeman and co-workers.[10,11] They used the full-potential linearized augmented-plane-wave (FLAPW) method to investigate the Ag/MgO(001) interface in a slab geometry, and found that the preferred adsorption site of the overlayer Ag atoms is on the O site of the clean MgO(001) surface. Li and Freeman[12] also investigated a 3d ferromagnetic metal-ceramic interface system, Fe/MgO(001), by the FLAPW method and found that the electronic and magnetic properties of a monolayer of Fe on MgO are remarkably close to that of a free-standing Fe monolayer, as a result of the lack of hybridization between Fe and MgO. Schönberger, Andersen, and Methfessel[13] carried out full-potential linearized muffin-fin orbital (FLMTO) calculations for Ti/MgO(001) and Ag/MgO(001) interfaces in a superlattice geometry, and found that both Ti and Ag also bind on top of oxygen and that the interface force constants for Ti/MgO are 3–4 times larger than that for Ag/MgO. Hong and co-workers[14,15] used the self-consistent local-orbital (SCLO) method to study Ag/MgO and Al/MgO systems, and found that the adsorption sites of both Ag in Ag/MgO(001) and Al in Al/MgO(001) are on the O site, and that all adhesion curves accurately obey the universal Harris function.[16] To explore the benign substrate for 4d monolayer magnetism, Wu and Freeman[17] investigated the structural, electronic, and magnetic properties of M/MgO(001) (M = Pd, Rh, and Ru) using the FLAPW method, and found that Ru and Rh monolayers retain large spin magnetic moments. According to their atomic force determinations, the metal overlayers are found to induce a significant buckling reconstruction in the interfacial MgO layer.

In this paper, we report results of first-principles FLAPW calculations for the Ag/CdO(001) system. We calculated the adsorption site of Ag, the equilibrium interfacial separation and the binding energy, and investigated the interface electronic structure in order to understand the binding mechanism of the metal–metal-oxide interface. As demonstrated in previous experiments and calculations for MgO as substrate, several types of interactions, such as ionic, covalent, and metallic bonding,

are involved in the interface. Their contributions to the binding are expected to vary with the materials involved. Here the important contributions in the Ag/CdO interface are identified by comparing the calculated electronic structure, such as the charge distribution, band structure and density of states (DOS), with that found previously for Ag/MgO.

II. COMPUTATIONAL MODEL AND METHODOLOGY

We set up a seven-layer slab model to study the Ag/CdO(001) interface which consists of a five-layer slab of CdO and a monolayer of Ag adsorbed on the CdO surface on each side of the slab. The lattice constants of Ag and CdO are set at the bulk values, and so the misfit is about 14%. Two symmetric adsorption sites of Ag atoms on the CdO(001) surface, i.e., above the O atom and above the Cd atom, are investigated. We calculated the total energy with respect to the interfacial separation between the Ag overlayer and the CdO interface layer to determine the site preference of Ag, the equilibrium distance, and the binding energy of the interface.

The highly precise FLAPW (Ref. 18) method with both van Barth-Hedin[19] and Hedin-Lundqvist[20] exchange-correlation energy was employed to solve the Kohn-Sham equations[21] self-consistently. Convergence is assumed when the difference between the input and output charge densities is smaller than 10^{-4} electrons/(a.u.^{3}). In the FLAPW method, no shape approximation is made for the charge density, potential, and matrix elements. The core electrons are treated relativistically, and the valence electrons are treated semirelativistically, i.e., the spin-orbit coupling is neglected. The muffin-tin (MT) radii of O, Cd, and Ag are set at 1.8, 2.2, and 2.3 a.u., respectively. We use 900 plane waves to expand the electronic wave functions in the interstitial region. The charge density and potential inside the MT sphere are expanded in spherical harmonics up to $l=8$, and 15 special k points in the $\frac{1}{8}$th irreducible two-dimensional (2D) Brillouin zone (BZ) are used to carry out the integrations.

III. RESULTS AND DISCUSSION

A. Calculated results

The total energy with respect to the interface separation, d, is calculated for Ag above the O and Cd sites and plotted in Fig. 1. The equilibrium separations for the O and Cd sites are 4.32 (2.28 Å), and 5.10 a.u. (2.70 Å), respectively. The binding energies are obtained by comparing the total energies of Ag/CdO, the CdO clean surface (determined from a separate five-layer calculation), and a free Ag monolayer. For Ag above the O site, the binding energy is 0.63 eV/atom; for Ag above the Cd site the binding energy is 0.29 eV/atom. Thus the Ag site preference is above the O atom. The calculated results are listed in Table I. It is interesting to compare our results for Ag/CdO(001) with that for Ag/MgO(001) by Li *et al.*[11] and Hong, Smith, and Srolovitz,[14] also listed in Table I. While the adsorption site for Ag is consistent with our results, the binding energies for Ag/MgO by Li *et al.* and by Hong, Smith, and Srolovitz are smaller than our result by 0.34 and 0.19 eV/atom, respectively. This clearly shows that the binding of the Ag/CdO interface is stronger than that of the Ag/MgO interface. Correspondingly, their equilibrium separations for Ag/MgO are larger than ours. The differences between the Ag/CdO and Ag/MgO interfaces are due to the interfacial oxidation of the Ag atoms through hybridization with the O electrons, which is discussed below.

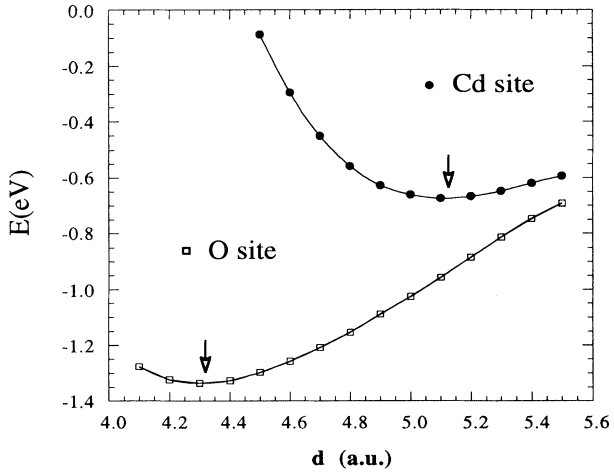

FIG. 1. Total energy vs distance for two positions of Ag on the CdO(001) surface: Ag above the O site and Ag above the Cd site.

As an ionic crystal, CdO has a very stable crystal structure, so the surface reconstruction due to the surface and the interface is expected to be small. We used both total-energy and force determinations to investigate the CdO surface reconstruction, and found that there is no buckling of O or Cd in the CdO interface layer.

B. Charge density

The charge-density contours in the (100) plane of the Ag/CdO slab (Ag above the O site), the CdO clean surface, and the free Ag monolayer are shown in Fig. 2. The difference of the charge densities, which is obtained by subtracting the Ag/CdO charge density from the superposed charge density of the CdO clean surface and the

TABLE I. Calculated binding energies and the equilibrium distances of the Ag/CdO(001) interface with Ag on O and Cd sites. Results for Ag/MgO(001) with Ag on O site in Refs. 11 and 14 are also listed for comparison.

System	Distance (a.u.)	Binding energy (eV)
Ag/CdO(O site)	4.32	0.63
Ag/CdO(Cd site)	5.10	0.29
Ag/MgO(O site)[a]	5.10	0.30
Ag/MgO(O site)[b]	4.42	0.44

[a]Li *et al.* in Ref. 11.
[b]Hong, Smith, and Srolovitz in Ref. 14.

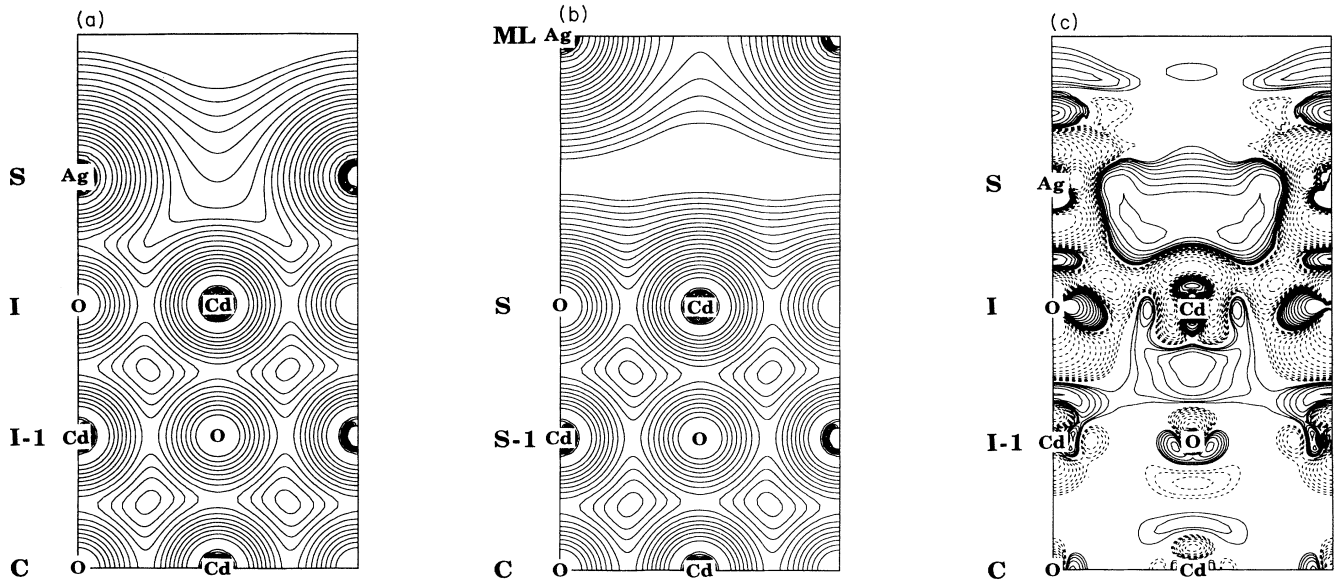

FIG. 2. (a) Charge density of Ag/CdO(001); (b) charge densities of the CdO(001) clean surface and the Ag monolayer; (c) charge-density difference, $\rho_{Ag/CdO}-\rho_{CdO}-\rho_{Ag}$, all in the (100) plane. In panels (a) and (b), contours start from 10^{-4} electrons/a.u.^{3} and increase successively by a factor of $\sqrt{2}$. In panel (c), solid lines denote the electron accumulation and the dashed lines denote electron loss, and contours start from $\pm 10^{-4}$ electrons/a.u.^{3} and change successively by a factor of $\sqrt{2}$.

Ag monolayer, is shown in Fig. 2(c). One can see that the charge distribution in the subinterface layer ($I-1$) and in the lower half of the interface layer (I) is similar to that in the bulklike center layer (C). Thus the interface effect is localized within the Ag overlayer and the interface layer of CdO, and decays rapidly into the CdO bulk. One can also see the screening in the interface from Fig. 2(c); where electrons accumulate in the area above the positively charged Cd atom.

Quantitatively, the charge population of each atom is listed in Table II along with the differences between the superposed monolayer and clean surface and the interface. Compared with the free Ag monolayer and the CdO clean surface, the populations of O and Cd atoms in the center and the subinterface layers remain essentially unchanged. The populations of Ag, O, and Cd atoms in the interface differ from the Ag monolayer and the CdO surface by 0.020, 0.039, and 0.009 electrons for the O site adsorption, and by 0.011, −0.008, and 0.014 electrons for the Cd site adsorption, respectively. Obviously, there is no significant charge transfer away from the interface.

C. Band structure

The band structures of the Ag monolayer, CdO surface, and Ag/CdO overlayer (with Ag above the O site) are shown in Fig. 3. The solid lines in the overlayer band structure denote states whose wave functions have more than 50% weight within the overlayer Ag atom. In the interface, the O s-p electron band is located from −1 to −5.8 eV below E_F, and the Ag 4d electron band is located about −3.7 eV below E_F. Compared with the Ag monolayer and CdO surface band structures, a remarkable change of the interface band structure happens at the top of the O s-p band at about −2 eV below E_F around the $\bar{M}$ point; this should appear as a very strong feature in photoemission spectra. In Ag/CdO, the energy level is shifted upward by about 0.9 eV and the valley at $\bar{M}$ is flattened. Dramatically, these states have more than a 50% Ag 4d component, but there is no corresponding Ag electron level at this place in the Ag monolayer, thus indicating that these states are the hybridized states between the Ag and O atoms in the interface layers.

TABLE II. Layer-by-layer charge population and charge transfer in their muffin-tin spheres. Charge transfers are calculated as differences in charge population between the surface or monolayer and the interface.

Atom	Ag	O(I)	O($I-1$)	O(C)	Cd(I)	Cd($I-1$)	Cd(C)
Free Ag or CdO slab	45.151	7.524	7.578	7.576	45.655	45.690	45.685
Ag/CdO (O site)	45.171	7.563	7.577	7.576	45.664	45.690	45.687
Charge transfer	0.020	0.039	−0.001	0.000	0.009	0.000	0.002
Ag/CdO (Cd site)	45.162	7.516	7.587	7.575	45.669	45.690	45.685
Charge transfer	0.011	−0.008	0.009	−0.001	0.014	0.000	0.000

D. Density of states

The layer-projected partial DOS is shown in Fig. 4. The solid lines are the DOS of the Ag/CdO interface (again with Ag above the O site), and the dashed lines are the DOS of the Ag monolayer and the CdO surface. The DOS of the O(C) and the O($I-1$) atoms resemble that of the clean CdO surface, indicating that these two layers do not participate considerably in the interfacial adhesion. The DOS of the O(I) atoms show a different behavior compared with that of the clean surface. The O(I) peak near the bottom of the valence bands is enhanced, and peaks near the top of the valence bands are lowered. Also, one can see that the O(I) atoms are metallized because the DOS is not zero at the Fermi level. By contrast, the DOS of the Ag overlayer changes significantly from that of the free monolayer; the peak dominated by the Ag 4d electrons is lowered and broadened due to the interfacial hybridization between Ag and O. Three additional peaks at about -5, -3, and -2 eV below E_F are formed near the top and bottom of the main Ag 4d peak. It is important to notice that peaks at these energies also exist in the O(I) DOS; this coexistence indicates that the additional peaks in the DOS of the Ag overlayer are actually the hybridized states between Ag and O(I). One can find that the peak at -2 eV below E_F corresponds to the hybridized states around $\bar{M}$ that we discussed above in the band structure. The Cd 4d states are located deep below the Fermi energy, so that even the surface Cd atoms do not play a significant role in Ag-CdO interaction.

To demonstrate the interfacial hybridization directly,

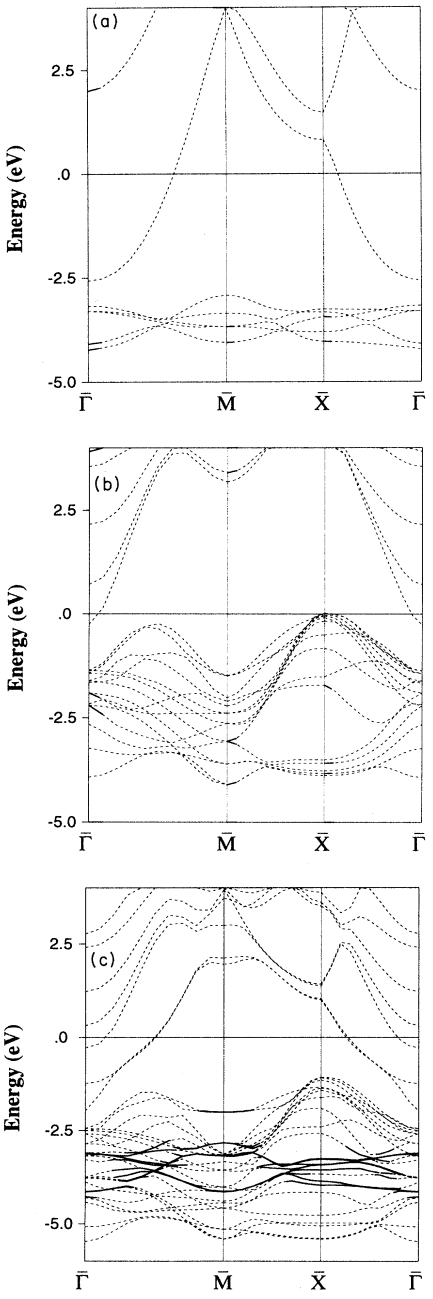

FIG. 3. Energy bands along high-symmetry directions in the 2D Brillouin zone for (a) the Ag monolayer, (b) the CdO(001) slab, and (c) the Ag/CdO(001) interface (Ag above O). Solid lines indicate states whose wave function has more than 50% weight within the overlayer Ag atom.

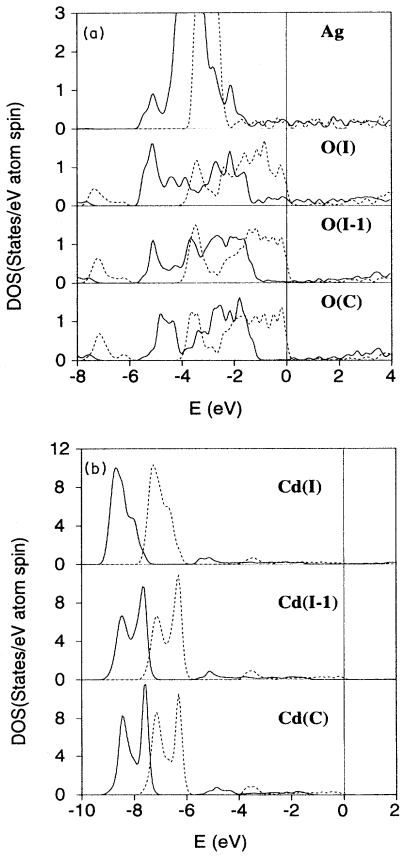

FIG. 4. The layer-projected density of states (DOS) of (a) Ag and O and (b) Cd. Solid lines are the DOS's of Ag/CdO(001) (Ag above the O site), and dashed lines are the DOS's of the free Ag monolayer and the CdO(001) slab.

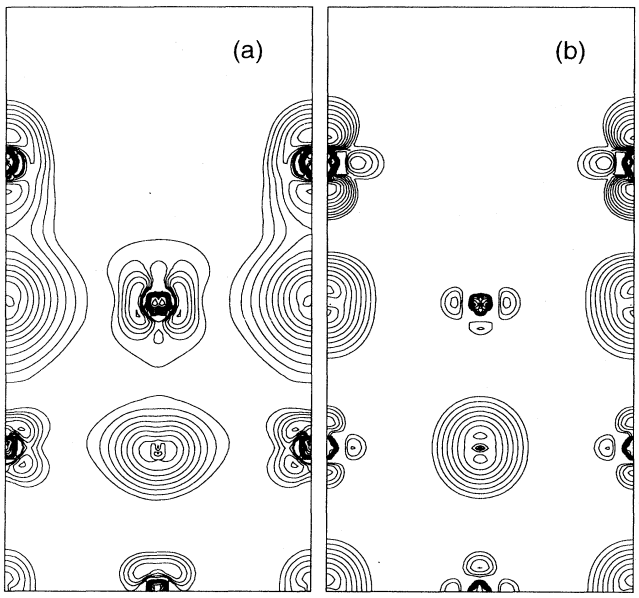

FIG. 5. The energy-sliced charge density in the energy range (a) from -5.2 to -5 eV below E_F, and (b) from -2.2 to -2 eV below E_F. Contours start from 10^{-3} electrons/a.u.^{3}, and increase successively by a factor of $\sqrt{2}$.

we cut energy slices at two of these peaks, one at -5 eV below E_F and one at -2 eV below E_F, each with a width of 0.2 eV, and plot their charge distributions in Fig. 5. The charge distribution of the energy slice at -5 eV below E_F shows that electrons accumulate in the region between Ag and O(I) and form p-d bonding states. The charge distribution of the energy slice at -2 eV below E_F shows that there is a depletion of electrons away from the region between Ag and O(I), and these states are p-d anti- bonding states. Thus the charge distributions illustrate the bonding and antibonding features of the electron states in the energy slices and provide direct evidence of the interfacial hybridization in the Ag/CdO interface.

As mentioned earlier, the binding energies of the Ag/MgO interface are found to be smaller than that of the Ag/CdO interface. We investigated the electronic structures of the Ag/MgO interface provided in Refs. 11 and 14, and found that there is no sizable coexistence of peaks in the DOS of the overlayer Ag and the interface O. Hence the interfacial hybridization in Ag/MgO is weaker than that in Ag/CdO, which explains why the binding energy of the Ag/CdO interface is larger than that of the Ag/MgO interface. For the same reason, the preferred adsorption site of Ag in the Ag/CdO interface is above the O site. This comparison of Ag/CdO and Ag/MgO demonstrates that although the antibonding states are also almost fully occupied, the interfacial hybridization between the Ag and O atoms makes a significant contribution to the adhesion of Ag/CdO system and plays an important role in this metal-ceramic interface. It also suggests why the CdO substrate is favorable for epitaxial growth (cf. the sharp interface found by Chan, Jang, and Seidman[9]), in contrast with the case of MgO.

ACKNOWLEDGMENTS

This work is supported by the U.S. Department of Energy (Grant No. DE-FG02-88ER45372) and by a grant of computing time on the NERSC supercomputer. We thank D. N. Seidman and K. Merkle for helpful discussions.

[1]See, e.g., *Metal-Ceramic Interfaces,* edited by M. Rühle, A. G. Evans, M. F. Ashby, and J. P. Hirth (Pergamon, Oxford, 1990).
[2]G. Fuchs, M. Treilleux, and P. Thevenard, Thin Solid Films **165**, 347 (1988).
[3]R. H. Hoel, Surf. Sci. **169**, 317 (1986).
[4]J. W. He and P. J. Möller, Surf. Sci. **180**, 411 (1987).
[5]J. W. He and P. J. Möller, Surf. Sci. **178**, 934 (1986).
[6]I. Alstrup and P. J. Möller, Appl. Surf. Sci. **33**, 134 (1988).
[7]K. H. Johnson and S. V. Pepper, J. Appl. Phys. **53**, 6634 (1982).
[8]Y. Park, Ph.D. thesis, Northwestern University, 1994.
[9]D. K. Chan, H. Jang, and D. N. Seidman, Scr. Metall. Mater. **29**, 1119 (1993).
[10]A. J. Freeman, C. Li, and C. L. Fu, in *Metal-Ceramic Interfaces* (Ref. 1), pp. 2–8.
[11]C. Li, R. Wu, A. J. Freeman, and C. L. Fu, Phys. Rev. B **48**, 8317 (1993).
[12]C. Li and A. J. Freeman, Phys. Rev. B **43**, 780 (1991).
[13]U. Schönberger, O. K. Andersen, and M. Methfessel, Acta Metall. Mater. **40**, S1 (1992).
[14]T. Hong, J. R. Smith, and D. J. Srolovitz, J. Adhesion Sci. Technol. **8-6**, 1 (1994).
[15]J. R. Smith, T. Hong, and D. J. Srolovitz, Phys. Rev. Lett. **72**, 4021 (1994).
[16]J. Harris, Phys. Rev. B **31**, 1770 (1985).
[17]R. Wu and A. J. Freeman (unpublished).
[18]E. Wimmer, H. Krakauer, M. Weinert, and A. J. Freeman, Phys. Rev. B **24**, 864 (1981).
[19]U. Von Barth and L. Hedin, J. Phys. C **5**, 1629 (1972).
[20]L. Hedin and B. I. Lundqvist, J. Phys. C **4**, 2064 (1971).
[21]W. Kohn and L. Sham, Phys. Rev. **140**, A1133 (1965).